REGIONAL EVENT IDENTIFICATION RESEARCH IN EASTERN ASIA

Xiaoning (David) Yang, Steven R. Taylor, Monica Maceira, Howard J. Patton, James T. Rutledge, George E. Randall and Marie D. Renwald

Los Alamos National Laboratory

Sponsored by National Nuclear Security Administration
Office of Nonproliferation Research and Engineering
Office of Defense Nuclear Nonproliferation

Contract No. W-7405-ENG-36

ABSTRACT

We describe ongoing studies of broad-area, regional-event identification in eastern Asia. The goal of our work is to provide a framework that allows for accurate identification, operational transparency, and clear reporting to nontechnical decision makers. The underlying methodologies need to have a clear physical basis packaged in a sound statistical framework having proper uncertainty estimates.

We are developing regional surface-wave discriminants (e.g., m_b - M_s) through a suite of focused studies. One of these studies is the development of surface-wave attenuation tomographic maps for central and southeast Asia. These maps can be used in the reformulation of regional M_s calculations with two-dimensional (2-D) path corrections to reduce station-magnitude scatter and network-magnitude bias. We have developed the 20-sec Rayleigh-wave attenuation map using a Bayesian inversion approach. *A priori* tomographic maps were constructed using two-station amplitude-ratio measurements. Single-station amplitude measurements were then inverted for higher resolution maps. In order to isolate and enhance the surface-wave signal, we applied phase-matched filters to the data before making spectral-amplitude measurements. The filtering proved to be effective in reducing the amplitude bias caused by multipathing and focusing. The average Q of the region estimated from the measurements is about 220, lower than most global estimates. The resultant tomographic map shows general correlation between the surface-wave attenuation pattern and the geology and tectonics of the region. Compared with one-dimensional (1-D) distance corrections, the use of 2-D attenuation model for path corrections in M_s calculations reduced the station-magnitude scatter by an average of 16 to 18 percent.

Another component of these studies involved evaluation and refinement of existing surface-wave slowness tomographic models. Slowness models at shorter periods (6 seconds and above) have been developed for central Asia. The development of these models is useful in lowering detection thresholds and allowing for discrimination at smaller magnitudes. Rayleigh-wave group-velocity dispersion curves were used to compute high-resolution, 0.5-degree cell size, slowness tomographic maps. We used a declustering technique to minimize the effect of event clusters on the inversion results. Patterns of the tomographic maps correlate well with known geologic and tectonic features in the area. Residual analysis with an independent set of group-velocity measurements showed significant improvement by the refined model compared with the *a priori* model especially at shorter periods. The refined model also showed a 15% improvement in the detection of surfaces waves with respect to previous 1-D models.

The Magnitude and Distance Amplitude Correction (MDAC) methodology is used to correct regional seismic amplitudes for propagation effects and earthquake source scaling. We correct amplitudes rather than predefining various phase ratios because all information is retained from which to construct discriminants. Because signals from explosions are highly dependent on near-source material properties and emplacement conditions, it is difficult to *a priori* select discriminants for uncalibrated regions. The MDAC approach adds much flexibility to the problem and allows for construction of numerous combinations of discriminants in a multivariate setting using Gaussian statistics. Recent research results involving analysis of the Borovoye Archive and associated processing challenges will be presented. Additionally, preliminary work on optimal amplitude measurements from regional arrays for regional discriminants and on developing discriminant transfer functions between newly operational stations and historic stations will be presented.

OBJECTIVE

The objective of this work is to provide methodologies and calibration parameters for robust regional-event identification at reduced magnitude thresholds.

RESEARCH ACCOMPLISHED

20-sec Rayleigh-Wave Attenuation Tomography

The $m_b - M_s$ relationship has proven to be an effective teleseismic discriminant. Extending its application to regional distances requires the extension of the M_s definition and regionalized path and station calibration. Inclusion of two-dimensional (2-D) path correction in regional M_s calculations has the potential to reduce the station-magnitude scatter and network-magnitude bias. To test the concept, we developed 20-sec Rayleigh-wave attenuation models for central and southeast Asia (15° - 65° N; 70° - 130° E). The following two steps were used in developing the attenuation model. First, two-station amplitude-ratio measurements, which were less affected by source-parameter error than single-station amplitude measurements, to obtain a coarse-grid (5° cell) model through a tomographic inversion. Second, we inverted for the final model (2° cell) with single-station amplitude measurements, which had much better path coverage. The coarse-grid model was used as the *a priori* model in the final inversion in a Bayesian approach (Tarantola, 1987).

The instrument-corrected surface-wave spectra can be expressed as

$$A_o(\omega, R) = S(\omega)G(R)P(\omega)B(\omega, R), \tag{1}$$

where $S(\omega)$ is the source spectrum; $G(R)$ is the geometrical spreading; $P(\omega)$ is the site-response effect and $B(\omega, R)$ is the apparent attenuation. ω is the angular frequency and R is the distance. The attenuation term $B(\omega, R)$ can be written as $B(\omega, R) = \exp(-\gamma(\omega)R)$, where γ is the attenuation coefficient. Equation (1) is linearized by taking natural logarithms of both sides of the equation. After the geometrical-spreading correction, the linearized version of equation (1) becomes

$$\ln A(\omega, R) = \ln S(\omega) + \ln P(\omega) - \gamma(\omega)R. \tag{2}$$

If two seismic stations lie on the same great-circle path that goes through a seismic source, the geometrical-spreading corrected amplitude ratio between the two stations is

$$\frac{A(\omega, R_1)}{A(\omega, R_2)} = \frac{P_1(\omega)}{P_2(\omega)} e^{\gamma(\omega)(R_2 - R_1)},$$

or in the logarithm domain as

$$\ln \frac{A(\omega, R_1)}{A(\omega, R_2)} = \ln P_1(\omega) - \ln P_2(\omega) + \gamma(\omega)(R_2 - R_1). \tag{3}$$

In the tomographic inversion, we discretized the last term in Equations (2) and (3) and grouped multiple observations together. In a matrix form, the problem is expressed as

$$\mathbf{d} = \mathbf{G}\mathbf{m}. \tag{4}$$

Using 20-sec Rayleigh-wave spectral amplitudes, we solve for the model $\mathbf{m}$, which contains discretized attenuation coefficients, site-response and source terms, with a maximum-likelihood method (Menke, 1989) as

$$\mathbf{m} = \mathbf{m}_0 + (\mathbf{G}^T\mathbf{C}_d^{-1}\mathbf{G} + \mathbf{C}_{m0}^{-1})^{-1}\mathbf{G}^T\mathbf{C}_d^{-1}(\mathbf{d} - \mathbf{G}\mathbf{m}_0), \tag{5}$$

where $\mathbf{m}_0$ is the *a priori* model, and $\mathbf{C}_d$ and $\mathbf{C}_{m0}$ are the data and *a priori* model covariance matrices respectively. Within this Bayesian framework, statistical characteristics of the data and the *a priori* information are utilized in the inversion to constrain the results and their uncertainty.

Surface-wave generation and propagation are affected by many factors such as source mechanism and location, path heterogeneity and site response (e.g., Mitchell, 1995). To make reliable attenuation estimation, it is critical to separate attenuation effects from source effects and elastic path effects to the maximum extent possible. To accomplish this, we employed the phase-match filtering technique (Herrin and Goforth, 1977) and incorporated available source and path information in the amplitude-measurement procedure. The process involved correlating the surface-wave data with the phase-matched filter, identifying and windowing the primary surface-wave arrival on the resulting crosscorrelation, convolving the windowed crosscorrelation with the phase-matched filter to obtain the cleaned data and Fourier transforming the cleaned data into the frequency domain. This technique effectively reduced the bias caused by multipathing and focusing. Other background noise was also reduced. An added benefit of the filtering process was that it smoothed the data spectrum so that no arbitrary smoothing, such as autocorrelation or moving average, was needed before making the measurement.

With the procedure described above, we made 4,398 single-station amplitude measurements from 324 events that occurred in the study region. Figure 1a shows the path coverage of the measurements and Figure 1b plots the Harvard Centroid Moment Tensor (CMT) and geometrical-spreading corrected amplitudes as a function of source-receiver distance. The linear trend of the data in Figure 1b reflects the effects of the medium attenuation. Straight-line fit of the trend yielded an average Q of about 221. This value is similar to the Q estimate from two-station amplitude ratios. The value is smaller than most global estimates, which range from 400 to 700 (cf. Rezapour and Pearce, 1998). The amount of offset from unity of the intersection between the y-axis and the fitted line, about 0.19 $\log_{10}$ unit, is comparable with the amount of systematic bias of the CMT moments found by Patton (1998) for central Asia.

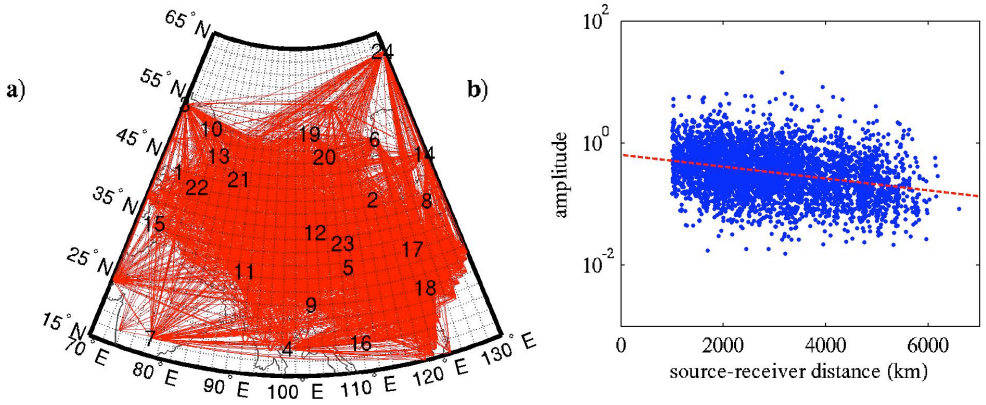

Figure 1. a) Path coverage of the single-station amplitude measurements. Station locations are marked by numbers. Grid lines define the discretization of the region for the final-model inversion. b) Source and geometrical-spreading corrected amplitudes as a function of source-receiver distance. Straight-line fit (dashed line) yielded an average *Q* of about 221.

With the results from the two-station amplitude-ratio inversion (Taylor *et al*., 2003) as the *a priori* model, we inverted the single-station spectral amplitudes using Equation 5 to obtain the final high-resolution 20-second Rayleigh-wave attenuation model together with site-response and source terms. Figure 2 presents the final model from the inversion. There is a broad correlation between the attenuation map and geologic and tectonic features of the region with low attenuation in cratonic regions (the Yangtze Craton, the Sino-Korean Craton and the Tarim Craton) and high attenuation in tectonically active regions (e.g., Tibetan Plateau). In Figure 2, the moment-magnitude data follow the line of linear correlation closely until the CMT magnitudes reach about 7.5. The CMT magnitudes then become larger than the corresponding magnitudes from the inversion, signaling magnitude saturation. The largest positive site-response term is for station BJT in northern China and the largest negative term is for station HYB in India.

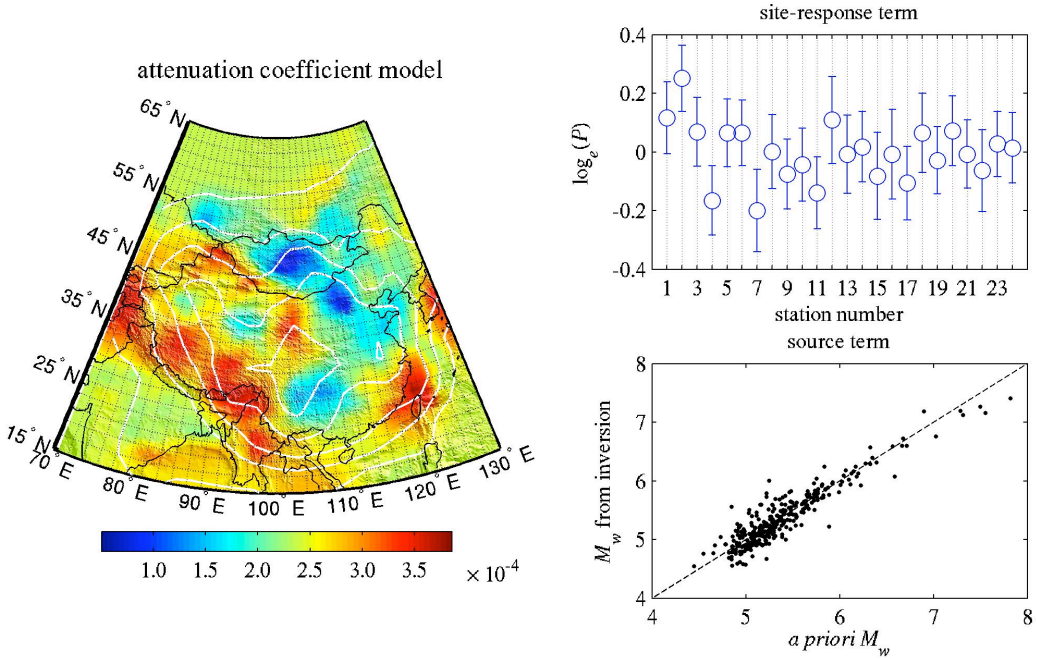

Figure 2. 20-second Rayleigh-wave attenuation-coefficient map, site-response and source terms from the single-station amplitude inversion. White contours in the attenuation map are isolines of one standard deviation of the map with smaller values in the middle of the map where path coverage was better. Site-response terms are displayed along with the error estimates. Station numbers correspond to those in Figure 1a. Source terms of the model are plotted as corresponding moment magnitudes against those from CMT.

One potential application of 2-D surface-wave attenuation maps is to make accurate distance corrections to amplitudes measured for M_s calculations. Current M_s formulae were defined for earthquakes at teleseismic distances (Gutenberg, 1945; Vanek et al., 1962; Rezapour and Pearce, 1998). A common feature of these formulae is the use of one-dimensional distance corrections. Because of the ever-improving station coverage of the Earth, surface-waves from smaller earthquakes are being recorded by an increasing number of regional stations, rendering the reliable regional M_s calculation possible. The use of regional 2-D attenuation models for distance corrections in regional M_s calculations is expected to reduce the scatter of the station magnitudes for an event and the network M_s bias.

In order to test the effectiveness of our model in reducing the station-magnitude scatter, an independent set of broadband data from 104 events was collected. We corrected the data for instrument response and band-pass filtered the data between 17 and 23 seconds. Then we measured the peak-to-zero amplitudes within the surface-wave window. By using Rezapour and Pearce's (1998) M_s formula, the average attenuation coefficient that we estimated from straight-line fitting of the spectral-amplitude data and the 2-D attenuation model from the inversion to apply different path-corrections to the amplitudes and estimated the station-magnitude variance reduction of the 2-D attenuation model. The maximum-likelihood value of the variance reduction is 32% when compared with Rezapour and Pearce's (1998) M_s formula and is 25% when compared with the constant attenuation model. The mean values of the variance reduction are 18% and 16% respectively. Considering the fact that another important cause of data scatter — the source radiation patterns, were not compensated for, we believe the amount of the variance reduction is significant.

Short-Period Rayleigh-Wave Slowness Tomography

Slowness models at short periods (6 seconds and above) have been developed for a region in central Asia. The development of these models is useful in lowering surface-wave detection thresholds and allowing for discrimination at smaller magnitudes.

We focus on the region of central Asia between 69° -108° E longitude and 29°-54° N latitude. Broadband waveform data from more than 1,100 events that occurred in the area between January 1997 and May 2002 was retrieved. Using multiple-filter analysis (Dziewonski *et al*., 1969; Herrmann, 1973) and phase-matched filter (Herrin and Goforth, 1977) techniques, we measured the dispersion characteristics of the signals. These Rayleigh-wave group velocity dispersion curves were used to compute high-resolution, 0.5° cell size, slowness tomographic maps for periods of 6, 8, 10, 12, 15, 18, 20, 22, 25, and 30 seconds.

A Bayesian tomography method (Tarantola, 1987) was adopted to solve the equation that relates the travel-time data with the velocity structure (Equation 4). Data and model parameters are considered independent and their covariance matrices are set to be diagonal. One of the advantages of using a Bayesian approach is that large-scale and well-accepted tomographic models from previous studies can be used as *a priori* background model. Global and regional 1° group-velocity maps were requested from different research groups (Levshin *et al*., 2001; Ritzwoller and Levshin, 1998; Stevens *et al*., 2001) and used as our background model.

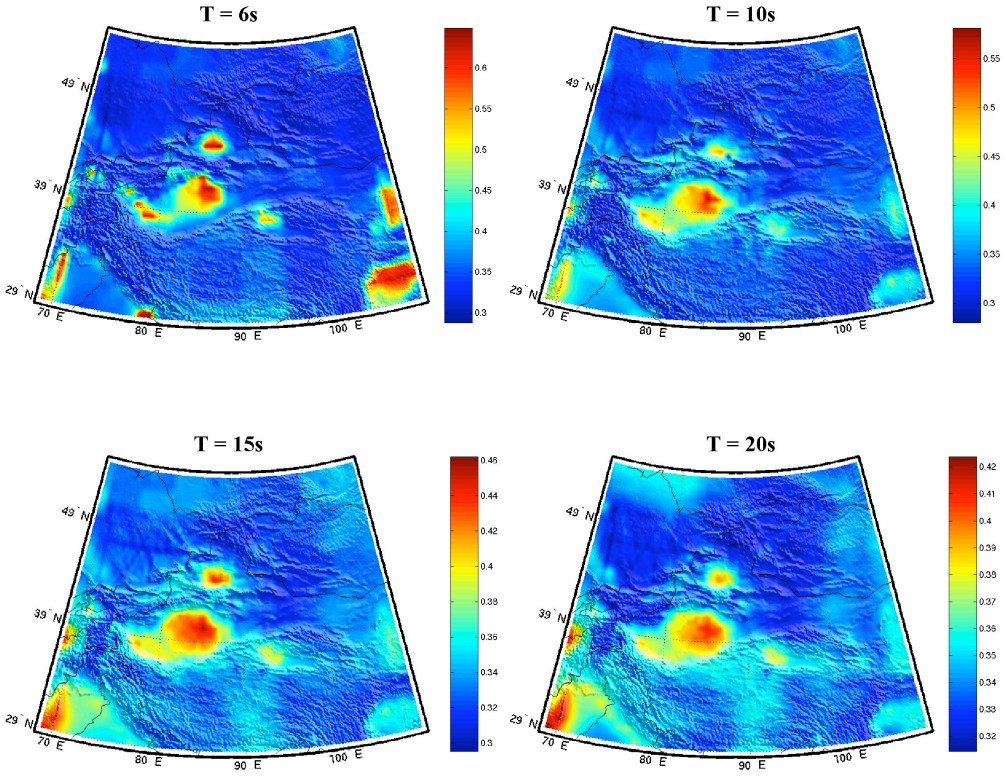

Figure 3. Rayleigh wave slowness maps for different periods. The slowness values are expressed in s/km and they are superimposed in a topographic map to ease the identification of plains and basins from mountains. Note that the color scale is different for each map.

We used a cell declustering technique (Isaaks and Srivastava, 1989) to remove the effect of event clusters. The cell declustering method uses the moving window concept to calculate how many measurements fall within particular regions or cells. Each measurement in a cell receives a weight that is inversely proportional to the number of events that fall within that cell.

Figure 3 gives some examples of the short-period slowness maps from the inversion. Patterns in our model correlate well with known geologic and tectonic features in the area. The short-period maps reflect the shallow part of the crust. The maps display low velocities associated with major sedimentary basins – Tarim, Junggar and Quaidam basins - in the area of central Asia under study. Higher velocities are associated with mountainous tectonic features such as the Tian Shan.

In order to test the effectiveness of our model, we collected an independent set of data that was not used in the computation of the slowness models, and measured the dispersion curves from the new data. Residual-analysis results for our slowness model and for the *a priori* model are shown in Figure 4. The overall map predictions are very good and, in general, better than the performance of the *a priori* model (plots a and c). The difference in performance is obvious at shorter periods (up to 15 seconds). Plots b and d include data for all periods, but the analysis of individual-period data yielded similar distributions. Their residual distributions are Gaussian-like with a mean close to zero (from –0.0219 km/s to +0.0202 km/s depending on the period) and with standard deviations ranging from 0.1810 to 0.2277 km/s. Considering all the periods together, most of the residuals have values between –0.5 and +0.5 km/s.

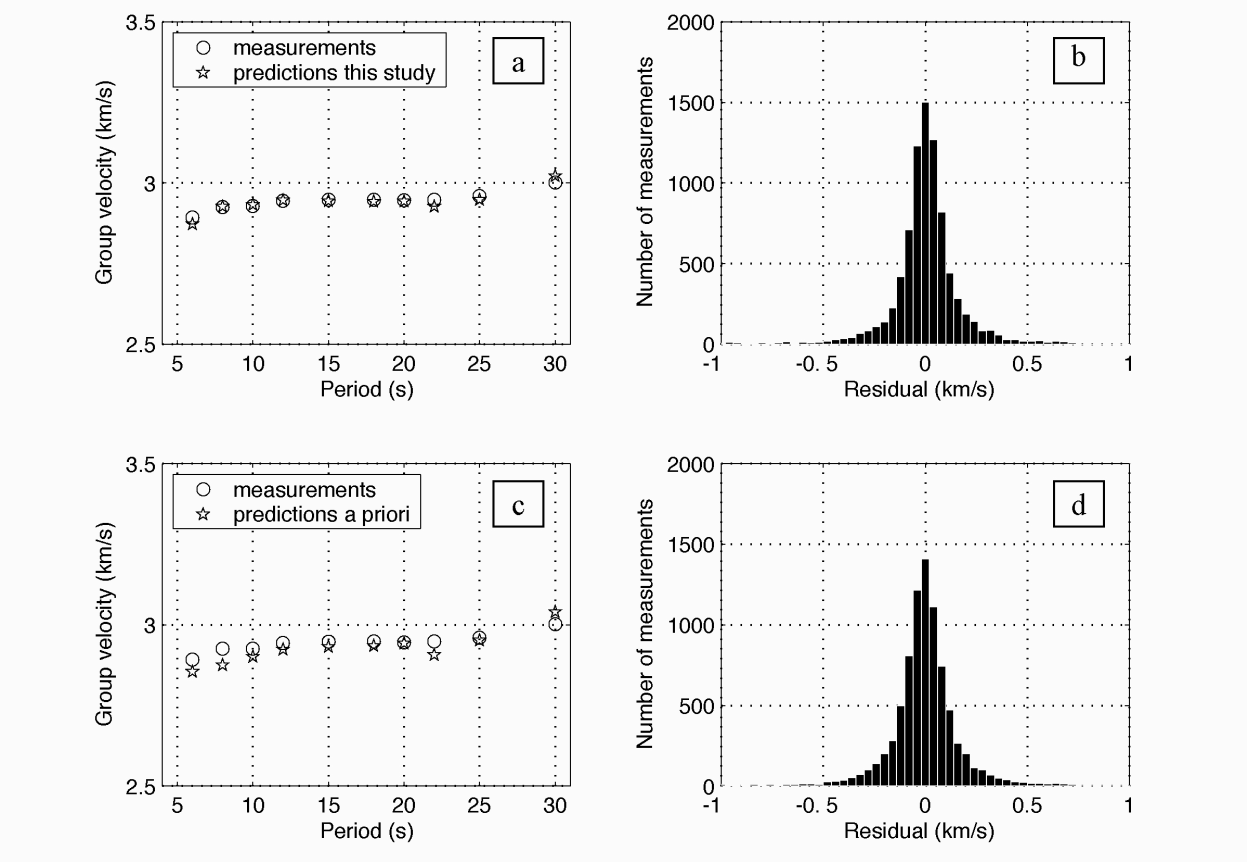

Figure 4. Residual analysis results. a) Average group velocities from the measurements and from slowness-model predictions. b) Distribution of the residuals obtained by subtracting the measurements from our model predictions. c) Average group velocities from the measurements and from the *a priori* model predictions. d) The same as b) with the predictions from the *a priori* model.

To evaluate the performance of our slowness model in detecting surface waves, we used Stevens and McLaughlin's (2001) surface-wave detection method and tested the improvement of our model against a one-dimensional (1D) China model (Jih, 1998) and the Preliminary Reference Earth Model (PREM from Dziewonski and Anderson, 1981). Figure 5 shows the number of surface wave detections using different velocity models. PREM and China 1D are the detection results using group velocity predictions calculated from the PRE, and from Jih's (1998) China crustal model. The use of our group velocity maps increased the number of surface wave detections by 15% with respect to using the China model.

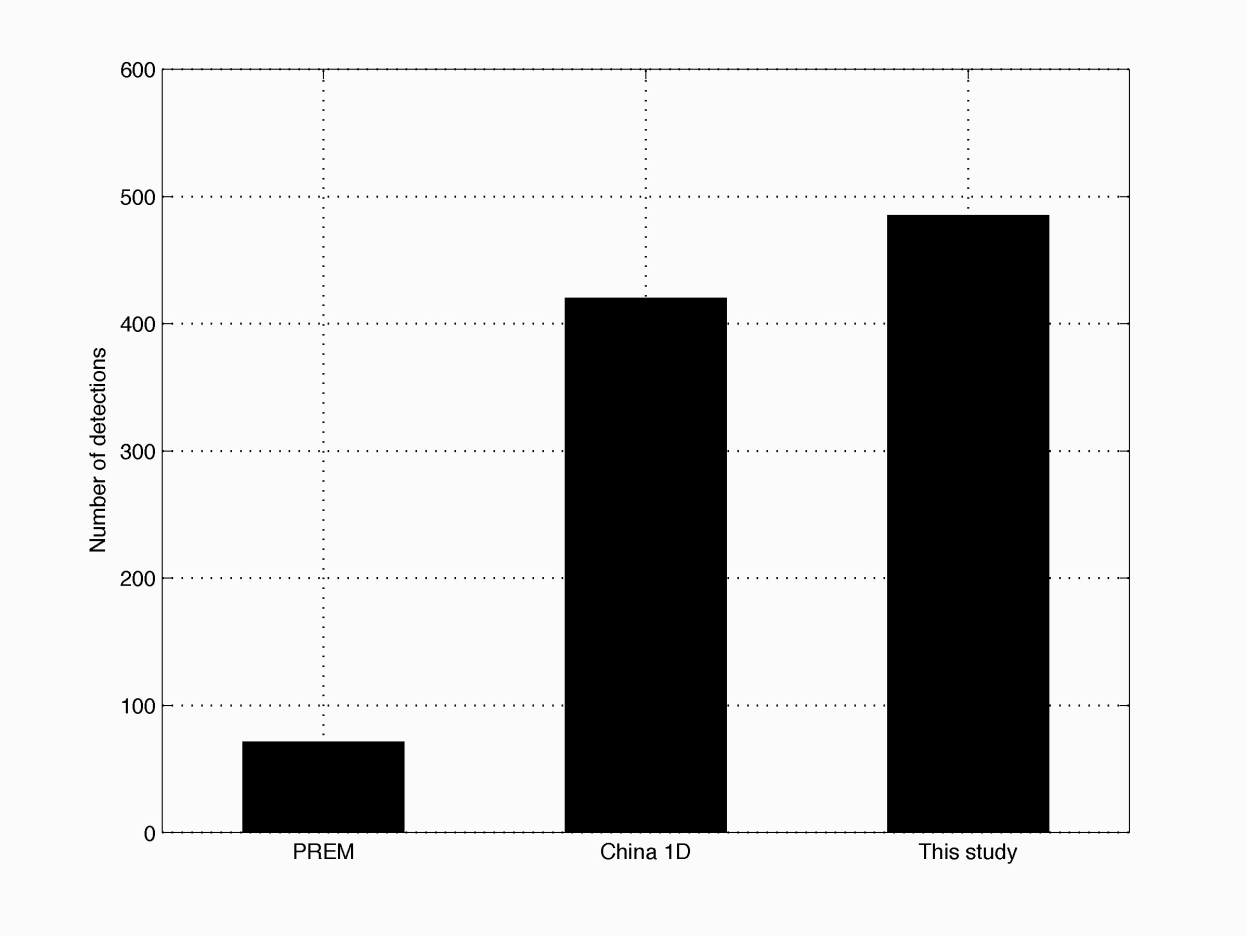

Figure 5. Number of surface wave detections using different group velocity models.

Magnitude and Amplitude Distance Corrections (MDAC)

A fundamental problem associated with event identification lies in deriving corrections that remove path and earthquake source effects on regional phase amplitudes used to construct discriminants. Our goal is to derive a set of physically based corrections that are independent of magnitude and distance, and amenable to multivariate discrimination by extending the technique described in Taylor and Hartse (1998) and Taylor *et al.* (2002). The MDAC procedure for correcting regional seismic amplitudes for seismic event identification has been modified to include more realistic earthquake source models and source scaling (MDAC2; Walter and Taylor, 2002).

The MDAC2 prediction of the observed, instrument-corrected spectra is similar to Equation 1:

$$A_m(\omega, R) = S(\omega)G(R)P(\omega)B(\omega, R). \tag{6}$$

We linearize both Equation 1 and Equation 6 by taking the logarithm of both sides and correct the observed spectrum by subtracting the log of MDAC2 spectrum

$$\log A_c(\omega, R) = \log A_o(\omega, R) - \log A_m(\omega, R). \tag{7}$$

These corrected spectra or residuals can then be kriged to further reduce un-modeled path effects (e.g., Schultz *et al.,* 1998).

For a given station and source region, a number of well-recorded earthquakes are used to estimate source and path corrections. In the MDAC2 formulation, the Brune (1970) earthquake source model is generalized with a more

physical apparent-stress model that can represent non-constant stress-drop scaling. We include a parameter that allows for variable P-wave and S-wave corner frequency scaling. The discrimination power in using corrected amplitudes lies in the assumption that the earthquake model will provide a poor fit to the signals from an explosion. The propagation model consists of a frequency-independent geometrical spreading and frequency-dependent power-law Q. Regional phase attenuation tomographic models are incorporated to replace a constant Q_0 model (Phillips *et al.,* 2000; Taylor *et al.,* 2003).

A grid search is performed simultaneously at each station for all recorded regional phases over stress-drop, geometrical spreading, and frequency-dependent Q to find a suite of good-fitting models that remove the dependence on M_w and distance. Very stable moment magnitude measures from regional coda wave envelopes that have been tied to independently derived regional seismic moments are incorporated. We also solve for frequency-dependent site/phase excitation terms. Once a set of corrections is derived, effects of source scaling and distance as a function of frequency are applied to amplitudes from new events prior to forming discrimination ratios. Thus, all the corrections are tied to M_w and distance and can be applied very rapidly in an operational setting. Moreover, phase-amplitude residuals as a function of frequency can be spatially interpolated (e.g., using kriging) and used to construct a correction surface for each phase and frequency. The spatial corrections from the correction surfaces can then be applied to the corrected amplitudes based only on the event location. The correction parameters and correction surfaces can be developed offline and entered into an online database for pipeline processing providing multivariate-normal corrected amplitudes for event identification illustrated in Figure 6.

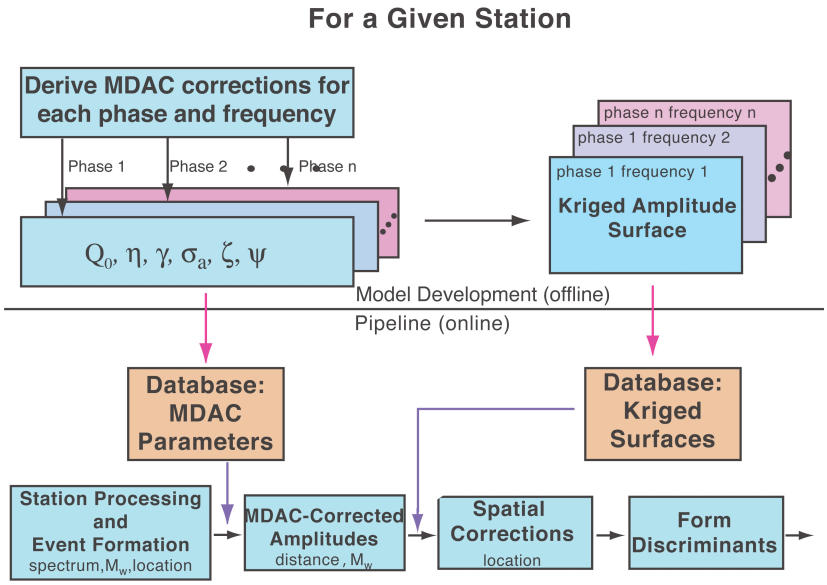

Figure 6. Example flowchart illustrating how the MDAC method can be combined with spatial interpolation (e.g., kriging) to develop database parameters to provide amplitude corrections for regional event identification in near-real time. These parameters can easily be incorporated into an operational pipeline to correct amplitudes from a new event for identification purposes.

CONCLUSIONS AND RECOMMENDATIONS

Event identification studies in Eastern Asia involve development of algorithms for constructing discriminants as well as applying the algorithms for station calibration. Our research, outlined in this paper, has focused on regional seismic discrimination using regional $m_b - M_s$ discriminants and MDAC corrected amplitudes. Ongoing work in the development of regional $m_b - M_s$ discriminants will build upon the surface-wave attenuation model and short-period surface-save slowness maps that we have developed.

ACKNOWLEDGEMENTS

We thank Anatoli Levshin and Michael Ritzwoller at the University of Colorado at Boulder, and Jeffry Stevens of Science Applications International Corporation (SAIC) for providing us with their surface-wave group-velocity models.

REFERENCES

Brune, J. N. (1970), Tectonic stress and spectra of seismic shear waves from earthquakes, *J. Geophys. Res.,* 75, 4997-5009.

Dziewonski, A. M., S. Bloch, and M. Landisman (1969), A technique for the analysis of transient seismic signals, *Bull. Seism. Soc. Am*., 59, 427-444.

Dziewonski, A. M. and D. L. Anderson (1981), Preliminary reference Earth model, *Phys. Earth Planet. Inter*., 25, 297-356.

Gutenberg, B. (1945), Amplitudes of surface waves and magnitudes of shallow earthquakes, *Bull. Seism. Soc. Am.*, 35, 3-12.

Herrmann, R. B. (1973), Some aspects of band-pass filtering of surface waves, *Bull. Seism. Soc. Am*., 63, 663-671.

Herrin, E. T. and T. T. Goforth (1977), Phase matched filters: application to the study of Rayleigh waves, *Bull. Seism. Soc. Am.*, 67, 1259-1275.

Isaaks, E. H. and R. M. Srivastava (1989), *An Introduction to Applied Geostatistics*, Oxford University Press, New York, 561 pp.

Jih, R. S. (1998), "Location Calibration Efforts in China", in *20th Annual Seismic Research Symposium on Monitoring a Comprehensive Test Ban Treaty (CTBT)*, pp. 44-55.

Levshin, A.L., M. H. Ritzwoller, M. P. Barmin, and J. L. Stevens (2001), "Short Period Group Velocity Measurements and Maps in Central Asia", in *Proceedings of the 23rd Seismic Research Review: Worldwide Monitoring of Nuclear Explosions*, pp. 258-269.

Menke, W. (1989), *Geophysical Data Analysis: Discrete Inverse Theory*, Academic Press, San Diego, California.

Mitchell, B. J. (1995), Anelastic structure and evolution of the continental crust and upper mantle from seismic surface wave attenuation, *Rev. of Geophys.*, 33, 441-462.

Patton, H. J. (1998), Bias in the centroid moment tensor for central Asian earthquakes: evidence from regional surface wave data, *J. Geophys. Res.*, 103, 26963-26974.

Phillips, W. S, H. E. Hartse, S. R. Taylor (2000), 1 Hz Lg Q tomography in central Asia, *Geophys. Res. Lett.,* 20, 3425-3428.

Rezapour, M. and R. G. Pearce (1998), Bias in surface-wave magnitude M_s due to inadequate distance corrections, *Bull. Seismol. Soc. Am.*, 88, 43-61.

Ritzwoller, M. H. and A. L. Levshin (1998), Eurasian Surface Wave Tomography: Group Velocities, *J. Geophys. Res.* 103, 4839-4878.

Schultz, C. A., S. C. Myers, J. Hipp, and C. Young (1998), Nonstationary Bayesian Kriging: A predictive technique to generate spatial corrections for seismic detection, location, and identification, *Bull. Seism. Soc. Am.,* 88, 1275-1288.

Stevens, J. L., D. A. Adams, and G. E. Baker (2001), Improved Surface Wave Detection and Measurement using Phase-Matched Filtering with a Global One-Degree Dispersion Model, in *Proceedings of the 23rd Seismic Research Review: Worldwide Monitoring of Nuclear Explosions*, pp. 420-430.

Stevens, J. L. and K. L. McLaughlin (2001), Optimization of Surface Wave Identification and Measurement, *Pure Appl. Geophys*., 158, 1547-1582.

Tarantola, A. (1987), *Inverse Problem Theory*, Elsevier Science, Amsterdam, The Netherlands, 630 pp.

Taylor, S. R. and H. E. Hartse (1998), A procedure for estimation of source and propagation amplitude corrections for regional seismic discriminants, *J. Geophys. Res.,* 103, 2781-2789.

Taylor, S. R., A. A. Velasco, H. E. Hartse, W. S. Phillips, W. R. Walter, and A. J. Rodgers (2002), Amplitude corrections for regional seismic discriminants, *Pure. App. Geophys*. 159, 623-650, 2002.

Taylor, S. R., X. Yang, W. S. Phillips, H. J. Patton, M. Maceira, H. E. Hartse, and G. E. Randall (2003), Regional event identification research in Eastern Asia, in *Proceedings of the 25th Seismic Research Review - Nuclear Explosion Monitoring: Building the Knowledge Base*, LA-UR-03-5017, Vol. 1, pp. 476-485.

Taylor, S. R., X. Yang, and W. S. Phillips (2003), Bayesian Lg attenuation tomography applied to eastern Asia, *Bull. Seism. Soc. Am.*, 93 795-803.

Vanek, J., A. Zatopek, V. Karnik, N. V. Kondorskaya, Y. V. Riznichenko, E. F. Savarensky, S. L. Solov'ev, and N. V. Shebalin (1962), Standardization of magnitude scales, *Bull. Acad. Sci. USSR, Geophys. Ser.*, no. 2, 108-111 (in English).

Walter, W. R. and S. R. Taylor (2002), A revised Magnitude and Distance Amplitude Correction (MDAC2) procedure for regional seismic discriminants: Theory and testing at NTS, *Los Alamos National Laboratory*, LA-UR-02-1008, 15pp.